

Influence of Capping Ligands on the Self-organization of Gold Nanoparticles into Superlattices from CTAB Reverse Micelles

LIN, Jun^{*a} (林君) ZHOU, Wei-Lie^b (周维烈) CARPENTER, Everett^b O'CONNOR, Charles^b

^aKey Laboratory of Rare Earth Chemistry and Physics, Changchun Institute of Applied Chemistry, Chinese Academy of Sciences, Changchun, Jilin 130022, China

^bAdvanced Materials Research Institute, College of Science, University of New Orleans, New Orleans, LA 70148, USA

Gold nanoparticles with size 3—10 nm (diameter) were prepared by the reduction of H₂AuCl₄ in a CTAB/octane + 1-butanol/H₂O reverse micelle system using NaBH₄ as the reducing agent. The as-formed gold nanoparticle colloid was characterized by UV/vis absorption spectrum and transmission electron microscopy (TEM). Various capping ligands, such as alkylthiols with different chain length and shape, trioctylphosphine (TOP), and pyridine are used to passivate the gold nanoparticles for the purpose of self-organization into superstructures. It is shown that the ligands have a great influence on the self-organization of gold nanoparticles into superlattices, and dodecanethiol C₁₂H₂₅SH is confirmed to be the best ligand for the self-organization. Self-organization of C₁₂H₂₅SH-capped gold nanoparticles into 1D, 2D and 3D superlattices has been observed on the carbon-coated copper grid by TEM without using any selective precipitation process.

Keywords gold nanoparticle, self-organization, capping ligands, reverse micelles

The use of metal and semiconductor nanoparticles as quantum dots in nanoelectronics demands their regular arrangement in three, two, or one dimension (3D, 2D, 1D), depending on the purpose.¹ Novel collective properties will be obtained due to the interactions of the individual nanoparticles in the ordered arrays.² So in recent years, more and more attention has been paid to the organization of these nanoparticles into ordered superlattices.³⁻¹⁰

Nanoparticles of gold colloids have been extensively

studied for a long time due to their unique physical, chemical properties and wide applications.¹¹ Since the first report on synthesis of thiol-derivatized gold nanoparticles in a two-phase liquid-liquid system in 1994 by Brust *et al.*,¹² several papers have been published on the synthesis and subsequent self-organization of gold nanoparticles into 2D and 3D superlattices by this method.^{13,14} Additionally, a gas-phase method followed by solution-phase encapsulation,¹⁵ A-B diblock polymer method¹⁶ have also been developed for the syntheses and self-organization of gold nanoparticles into superlattices. In most of above cases, the gold nanoparticles are capped by alkylthiols and have a narrow size distribution. Interestingly enough, self-organization of two distinct sized gold nanoparticles into ordered raft has been reported by Kiely and coworkers recently.¹⁷ Although the alkylthiols are widely used as capping ligands for the gold nanoparticles, there is still lack of a systematic study of the influence of different thiols and other ligands on the self-organization of gold nanoparticles. Furthermore, a simple manufacturing method of ordering nanoparticles in arrays of macroscopic dimensions is needed. So in the present paper, a detailed study on the synthesis and subsequent self-organization of gold nanoparticles into superstructures under various ligand conditions in a CTAB (cetyltrimethylammonium bromide) reverse micelle system is reported. The self-organization of gold nanoparticles is simply performed without

* E-mail: jlin@ns.ciac.jl.cn

Received September 17, 2001; revised October 15, 2001; accepted October 22, 2001.

Project supported by the Advanced Materials Research Institute at University of New Orleans through Defense Advanced Research Projects Agency (No. MDA972-97-1-0003) and the Hundred-Person Project of Chinese Academy of Sciences.

any selective precipitation and washing procedures. 1D nanowires, relatively large areas of ordered 2D nanorays, and 3D multilayers have been achieved by properly capping the gold nanoparticles, and their formation mechanisms are also discussed in the context.

Experimental

The starting materials for the synthesis and self-organization of gold nanoparticles were hydrogen tetrachloroaurate(III) trihydrate $\text{HAuCl}_4 \cdot 3\text{H}_2\text{O}$ (Aldrich), sodium borohydride NaBH_4 (99.995%, Aldrich), cetyltrimethylammonium bromide (CTAB, Aldrich), octane (Aldrich, 99%, anhydrous), 1-butanol (Aldrich, 99%), toluene (Aldrich), distilled water (self-made), and various dispersants such as trioctylphosphine [$\text{CH}_3(\text{CH}_2)_7$] $_3\text{P}$ (TOP, Aldrich, 90%), pyridine $\text{C}_5\text{H}_5\text{N}$ (Aldrich), 1-dodecanethiol $\text{CH}_3(\text{CH}_2)_{11}\text{SH}$ (98%, Aldrich), 1-octadecanethiol $\text{CH}_3(\text{CH}_2)_{17}\text{SH}$ (Aldrich), cyclohexyl mercaptan $\text{C}_6\text{H}_{11}\text{SH}$ (97%, Aldrich), 1-hexanethiol $\text{CH}_3(\text{CH}_2)_5\text{SH}$ (95%, Aldrich), dioctyl sulfide [$\text{CH}_3(\text{CH}_2)_7$] $_2\text{S}$ (96%, Aldrich) and 1,6-hexanedithiol $\text{HS}(\text{CH}_2)_6\text{SH}$ (96%, Aldrich). All the chemicals were used without further treatment except that octane, 1-butanol and distilled water were degassed by bubbling with dry argon gas for 3 h prior to the experiment. The degassing process is a necessary step for a well-controlled growth of nanoparticles. Gold nanoparticles were prepared by the reduction of HAuCl_4 in CTAB/octane + 1-butanol/ H_2O reverse micelle system using NaBH_4 as the reducing agent. First the phase diagram of CTAB/octane + 1-butanol/ HAuCl_4 (0.056 mol/L aqueous solution) reverse micelle system was established by a progressive dilution method. The weight ratio of the octane (oil) to cosurfactant (1-butanol) was kept at 4:1 (w/w) for all measurements. A combination of this homogeneous mixture was then treated as a single (pseudo-) component in the ternary phase diagram. Twenty compositions of CTAB and octane + 1-butanol (whose weight ratio is from 0.023 to 0.065) were selected, then HAuCl_4 aqueous solution was added in steps to each composition under agitation. The weights of HAuCl_4 aqueous solution in the boundaries from turbid phase to homogeneous phase and from homogeneous phase to turbid phase were recorded. In this way the phase diagram of CTAB/octane + 1-butanol/ HAuCl_4 (0.056 mol/L aqueous) system was established.

The preparation of gold nanoparticles was tried under two kinds of experimental environments, *i. e.*, one is under dry argon gas and another is under ultrasonic agitation. In a typical experiment, 0.3 g of CTAB, 0.148 mL of 0.056 mol/L HAuCl_4 aqueous solution, 1.0 g of octane (surfactant) and 0.25 g of 1-butanol (cosurfactant) were mixed together and stirred vigorously for 10 min until a homogenous phase was obtained [called reverse micelle a]. Reverse micelle b was prepared in the same way except that the HAuCl_4 solution was replaced by the same volume of 0.32 mol/L NaBH_4 aqueous solution. In this way the water/surfactant molar ratio (w) was kept at constant of 10 in the whole micelle system. Reverse micelle b was slowly added to reverse micelle a under argon gas bubbling or under ultrasonic agitation. A dark-red color was developed with gas releasing during this process, indicating the occurrence of the oxidation-reduction reaction and the formation of the gold colloid. Due to the high stability of the gold colloid, its color remained unchanged for several months. TEM results show that the size distribution of gold nanoparticles is more homogeneous under ultrasonication than under argon gas bubbling. This is in agreement with the previously reported results.¹⁸ So ultrasonication was used in the whole experimental process.

The self-organization experiments were performed as follows. 1 mL aliquot of the as-formed gold colloid was taken out and transferred to a 20 mL vial. A certain amount (0.5–1.0 mL) of the above mentioned dispersants such as various alkylthiols, trioctylphosphine (TOP) or pyridine was added into this vial, respectively. This immediately resulted in the formation of precipitates. In this way, most of the gold nanoparticles were extracted from the reverse micelle system due to the affinity of the dispersants with gold. The addition of 13.5–14.0 mL of toluene or heptane into the precipitates and subsequent ultrasonication for 40 min led to partly dissolving the precipitate, *i. e.* the formation of a suspension. This suspension was placed on table overnight, yielding a clear and homogeneous red-purple supernatant (not all the case) and a black precipitate. The supernatant mainly contained the smaller dispersant-capped gold nanoparticles dissolved in toluene or heptane, as well as small amount of other organic precursors. The precipitate mainly consisted of larger dispersant-capped gold particles (black) and CTAB, which are not dissolved in toluene or heptane. The supernatant

was characterized by absorption spectra and used to form superlattices of gold nanoparticles. Self-organization of gold nanoparticles into superlattices was performed by evaporation of the above-prepared gold supernatant on carbon-coated copper grids.

TEM study was performed on a JEOL 2010 transmission electron microscope. From the TEM micrographs the size distributions of different samples were determined. UV/vis absorption spectra were recorded on a CARY 500 Scan UV-vis-NIR spectrophotometer.

Results and discussion

Phase diagram and gold nanoparticle formation

Fig. 1 shows the pseudo-ternary diagram (in wt%) for the CTAB-octane (80%) + 1-butanol (20%)- HAuCl_4 (0.056 mol/L aqueous solution) system. The hatched area on the top of the diagram stands for a homogeneous single phase (micelle) region. The other unmarked area in the phase diagram stands for two or three turbid phases or gel phase (not labeled). The shape of the micelle region in the diagram is basically in agreement with that of CTAB-heptane-water system reported before.¹⁹ The micelle compositions for the experiments were determined according to this phase diagram.

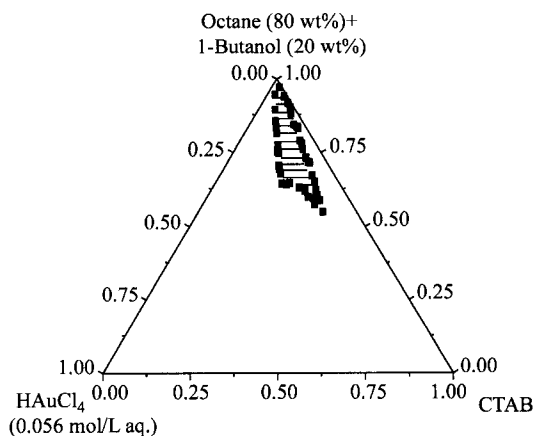


Fig. 1 Phase diagram (in wt%) of CTAB-octane + 1-butanol- HAuCl_4 aqueous solution system at room temperature.

The formation of metallic gold(0) nanoparticles from the reduction of HAuCl_4 by NaBH_4 can be verified by the UV/vis absorption spectrum and TEM. Fig. 2

shows the UV-visible absorption spectrum of the as-formed black colloid diluted by octane. A well-defined surface plasmon absorption band ranging from 400 to 700 nm with a maximum value at 524 nm is observed. According to the reported results,¹⁸ this is undoubtedly attributed to nanosized metallic gold particles. Further characterization was carried out by TEM. The corresponding TEM micrograph and histogram of the as-formed colloid (diluted by octane) are shown in Fig. 3, respectively. Many spherical particles with diameter ranging from 3 to 10 nm can be seen clearly from this micrograph. The electron diffraction pattern (inset of Fig. 3) reveals a crystalline order. The diffraction rings (from inside to outside) correspond to the (111), (200), (220) and (311) FCC metallic gold diffraction, respectively.

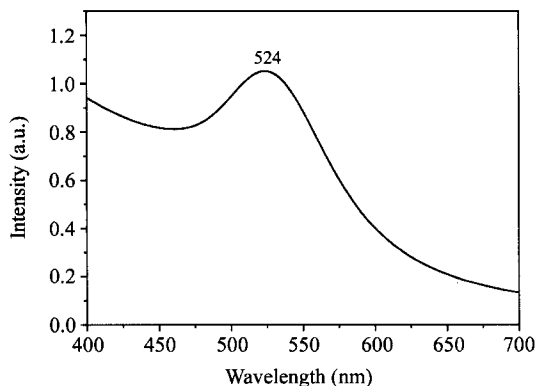


Fig. 2 UV-visible absorption spectrum of the as-formed gold colloid diluted by octane.

Influence of different ligands on the self-organization of gold nanoparticles

Due to the high polydispersity (3–10 nm) of the as formed gold particles, they could not form ordered superstructure (as shown in Fig. 3). The surface modification of metallic gold particles with organic ligands is able to prevent from their growth and aggregation, thus increasing their long term stability. This plays an important role in the self-organization of gold nanoparticles into superlattices. Here we select several alkylthiols (including dithiol and sulfide) with different alkyl chain lengths and shapes, trioctylphosphine (TOP) and pyridine as ligands of gold nanoparticles, to study their influence on the self-organization into superlattices. The

experimental results confirm that the ligands indeed have great influence on the characters of self-organization of gold nanoparticles into superlattices. The main results are listed in Table 1.

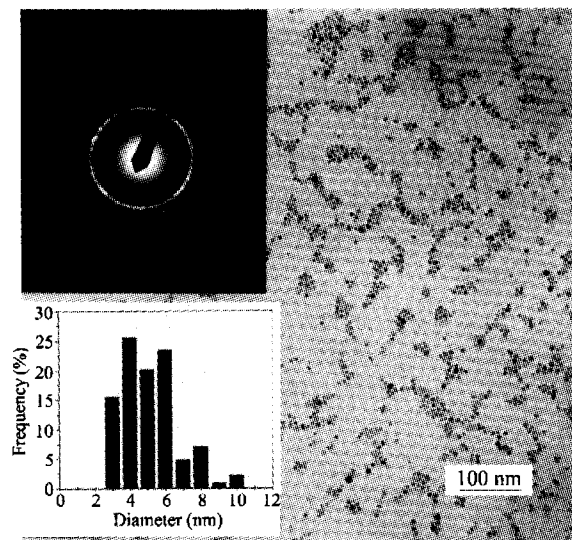
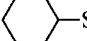


Fig. 3 TEM micrograph of the as-formed gold particles in CTAB reverse micelle (diluted by octane). The inset shows the electron diffraction pattern and histogram of gold nanoparticles.

Table 1 Influence of various ligands on the self-organization of gold nanoparticles and maximum values in absorption spectra of gold colloids using toluene as solvent

Ligands for gold nanoparticles	λ_{\max} (nm)	Characteristics of superstructures ^b
C_5H_5N (pyridine)	521 ^a	2D + 3D (disordered)
$[CH_3(CH_2)_7]_3P$ (TOP)	518	no superstructure
$CH_3(CH_2)_5SH$	525	3D (disordered)
 -SH	525	3D (disordered)
$HS(CH_2)_6SH$	—	2D + 3D (disordered)
$[CH_3(CH_2)_7]_2S$	522	2D (ordered)
$CH_3(CH_2)_{11}SH$	523	1D, 2D, 3D (ordered)
$CH_3(CH_2)_{17}SH$	—	no superstructure

^a Using heptane as solvent (the particles are not dissolved in toluene). ^b 1D; one-dimensional nanowire; 2D; two-dimensional nanoarray (monolayer); 3D; three-dimensional superlattice (multilayer).

The addition of pyridine (C_5H_5N) ligand to the as-formed gold colloid results in the formation of dark gray-

ish precipitate, which is completely insoluble in toluene but partially soluble in heptane. Fig. 4 shows the TEM micrograph and histogram for the pyridine-capped gold nanoparticles (from the heptane solution). Different from the formation of many smaller islands shown in Fig. 3, a larger area of monolayer (two-dimension, 2D) of gold nanoparticles is observed in Fig. 4. However, the dispersity of the gold nanoparticles is still high (3.0–8.8 nm as indicated by the histogram in Fig. 4) and the ordering is not good. Additionally, in the central part of the monolayer, formation of bilayer (3D) which appears as overlapping contrast, can be observed. TOP-capped gold nanoparticles can be dissolved in toluene. TEM results reveal that these gold particles are randomly distributed on the grid without any superstructure formation. The above results can be attributed to the lower affinity of phosphorus (P) and nitrogen (N) with Au. The gold nanoparticles can not be well passivated by TOP and pyridine, resulting in a random distribution (TOP-Au) or poorly ordered superstructure (2D + 3D, C_5H_5N -Au).

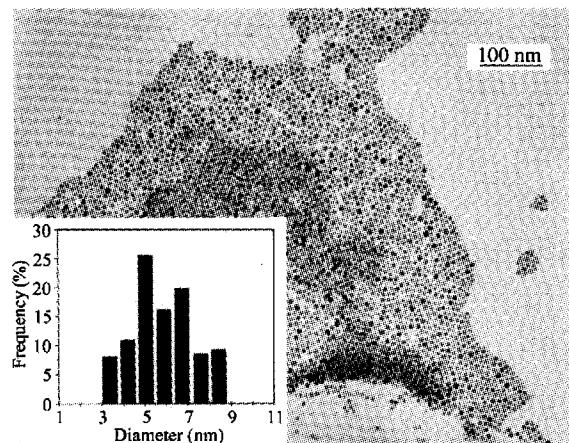


Fig. 4 TEM micrograph of pyridine C_5H_5N -capped gold nanoparticles obtained from heptane solution. The inset shows the histogram of gold nanoparticles.

For the ligands of alkanethiol series, it is observed that the shape and length of the carbon chains of the ligands have a great influence on the superstructures of the gold nanoparticles. For the gold nanoparticles capped by ligands with the short straight chain $[CH_3(CH_2)_5SH]$ and cyclohexyl mercaptan $C_6H_{11}SH$, mainly disordered 3D aggregation (multilayer) was observed on the TEM grids. This is because the chains of the ligands are too

short to prevent the gold nanoparticles from aggregation. The 1,6-hexanedithiol $\text{HS}(\text{CH}_2)_6\text{SH}$ can be used as a linking agent, which can connect two gold nanoparticles together according to its structural character (two sulfur head groups). Fig. 5 shows the TEM micrograph of $\text{HS}(\text{CH}_2)_6\text{SH}$ capped gold nanoparticles. Here it is difficult to distinguish the gaps among gold nanoparticles, clearly indicating that the gold nanoparticles are combined each other randomly and form a disordered 2D and/or 3D network. This may result from the rapid combination of gold nanoparticles by the hexanedithiol in various directions.

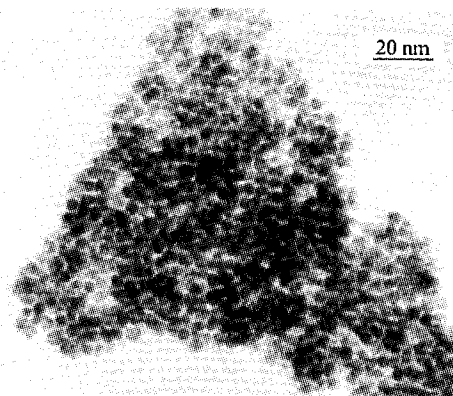


Fig. 5 TEM micrograph of $\text{HS}(\text{CH}_2)_6\text{SH}$ -capped gold nanoparticles obtained from toluene solution.

With increasing the number of carbon atoms to eight in the straight chains of the ligand $[\text{CH}_3(\text{CH}_2)_7]_2\text{S}$, a larger area of ordered 2D nanoarray (pure monolayer) has been observed, as shown by the TEM micrograph in Fig. 6. From this pattern it can be seen that homogeneous gold nanoparticles are organized in a hexagonal closed packed network accompanied by several obvious defects (blank region not covered by particles). The total area of the monolayer of gold nanoparticles is estimated to be $0.4 \mu\text{m}^2$. The most perfect superlattices are obtained when using alkanethiol with even longer carbon chain length $\text{CH}_3(\text{CH}_2)_{11}\text{SH}$ as the ligand for gold nanoparticles (as discussed later). It is shown that $n\text{-C}_{12}\text{H}_{25}\text{SH}$ is a very suitable ligand for passivating the gold nanoparticles, leading to the formation of ordered superlattices. In fact, the dodecanethiol $\text{C}_{12}\text{H}_{25}\text{SH}$ is well known to form self-assembled monolayer on planar gold substrates, which has been extensively studied.²⁰ However, further increasing the carbon chain length of the alkanethiol, namely, using $\text{CH}_3(\text{CH}_2)_{17}\text{SH}$ as ligand for gold nanoparticles yields a random distribution of gold

nanoparticles on the grid. This can be ascribed to the larger steric repulsive forces among $\text{CH}_3(\text{CH}_2)_{17}\text{SH}$ -capped gold particles caused by the longer alkane chains.

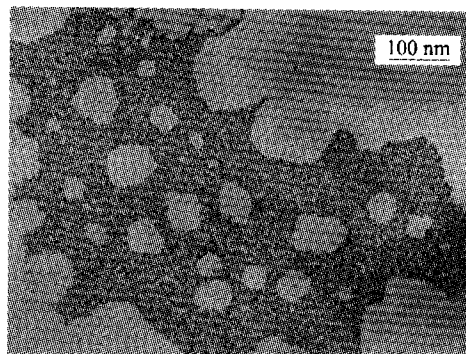


Fig. 6 TEM micrograph of $[\text{CH}_3(\text{CH}_2)_7]_2\text{S}$ -capped gold nanoparticles obtained from toluene solution.

Additionally, some spectral shifts are observed on the maximum absorption values of the gold colloids coated by these ligands, *i. e.*, from TOP-Au (518 nm) via pyridine-Au (521 nm) to sulfide-Au (522) and alkylthiol-Au (523—525 nm), as shown in Table 1. These spectral shifts may arise from the change in the free electron density or different size distribution of the gold colloids capped by these different ligands.⁸ Since the best superstructures are obtained in $\text{C}_{12}\text{H}_{25}\text{SH}$ -capped gold nanoparticles, more detailed studies will be performed on this system in the next section.

Two concentrations of $\text{C}_{12}\text{H}_{25}\text{SH}$ were tried to study the self-organization of gold nanoparticles: 0.5 mL and 1.0 mL of $\text{C}_{12}\text{H}_{25}\text{SH}$ were each added to 1 mL of the as formed gold colloids, which were then diluted to an equal volume (15 mL) by toluene. The superstructures of the gold nanoparticles obtained from these two different volume ratios (r) of $\text{C}_{12}\text{H}_{25}\text{SH}/\text{Au}$ colloid were examined in detail with TEM.

When $r = 0.5$, three kinds of superstructures, *i. e.*, one-dimensional nanowire (1D wire), two-dimensional nanoarray (2D monolayer) and three-dimensional superlattice (3D multilayer) were observed, as shown in Fig. 7(a), (b) and (c), respectively. It is interesting to find the formation of a 1D nanowire of gold clusters in the current system. The wire has a length about $1 \mu\text{m}$. The average size (diameter) of the gold nanoparticles in the wire is about 5.3 nm, and the nearest center-to-center distance between the clusters is 7.5 nm. This leads

the gap between two particles to be about 2.2 nm. So far several papers^{6,21} have been published on the formation of nanowires of metal colloids, most of which are produced by the template assistance. Generally speaking, the formation of nanowires without a template is not energetically favorable. There are two main reasons to form the Au nanowire in our case. One is that the carbon film used might have wrinkles which might act as a template to assemble nanocrystals into a wire array. Another is that the excess organic components (surfactant, cosurfactant and excess alkanethiol) left in that self-assembling zone might play some role in the formation of this feature, based on the fact that no such nanowire is found without the organic components.

The most frequently observed superstructure is an ordered 2D array of gold nanoparticles [Fig. 7(b)]. Nearly monodispersed spherical gold nanoparticles with diameters in the 5.0–6.7 nm range (and thus containing some 3800 to 9200 Au atoms, calculated according to Ref. 22) formed a closely packed hexagonal array, with one particle surrounded symmetrically by other six particles (*i. e.*, six-fold symmetry). This structural characteristic has been confirmed by the electron diffraction pattern, where the diffraction ring shows a hexagonal symmetry in contrast, as shown in the inset of Fig. 7(b). The image is dominated by the plane-projected arrangement of the nanocrystal cores because of the much greater scattering power of Au over the lighter elements (S, C, H).⁷ The histogram in Fig. 7(b) clearly shows a very narrow size distribution in this case, which favors the spontaneous organization of nanosized gold particles. The formation of hexagonal 2D gold nanoarray can be attributed to the equilibrium built between the van der Waals attractive forces and the steric repulsions from the thiol carbon chains (on the gold nanoparticles). Because these forces are isotropic, this equilibrium yields a compact organization in hexagonal 2D network.⁸ Similar to the 1D nanowire, the average size of the gold nanoparticles in the 2D array is about 5.8 nm, and the average center-to-center distance between adjacent clusters is 8.1 nm. So the average gap between two clusters is 2.1 nm. The length of the dodecanethiol C₁₂H₂₅SH tail is estimated to be 1.77 nm.⁸ Because the gold nanocrystals in this system are covered basically by a monolayer of dodecanethiol (the organic ligand layers can not be observed by TEM as indicated above, 1.77 nm × 2 = 3.54 nm > 2.2 nm), the alkyl thiols attached to adjacent gold

particles interpenetrate in the regions between the particles, forming the interdigitative bonding.³

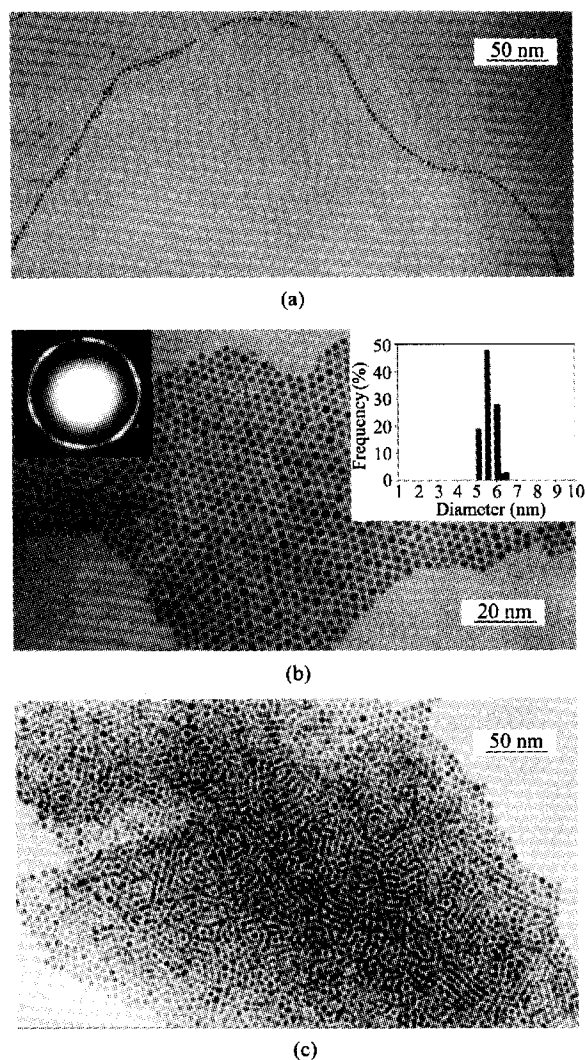


Fig. 7 TEM micrographs of C₁₂H₂₅SH-capped gold nanoparticles obtained from toluene for the volume ratio of C₁₂H₂₅SH/Au colloid $r = 0.5$. (a) 1D nanowire, (b) 2D nanoarray, (c) 3D superlattice. The insets in (b) show the electron diffraction pattern and histogram of gold nanoparticles.

Apart from the 1D and 2D superstructures, 3D superlattices are also found, as shown in Fig. 7(c). The formation of 3D superlattices can be resolved by careful examination of the TEM micrograph. At the edge of the self-assembly pattern, it is easy to see the hexagonal-close-packed 2D array of gold nanoparticles. Great difference in electronic contrast can be observed between the central part and the edge of the pattern, suggesting

the formation of multilayer. In the second layer, chain arrangements of the gold nanoparticles, which appear as straight lines or ring structures, can be seen clearly. The same structural pattern has been observed by Fink *et al.*,²³ which is attributed to the preference of occupying a 2-fold saddle site between two particles in the first layer rather than 3-fold hollow site created where three basal plane particles meet.

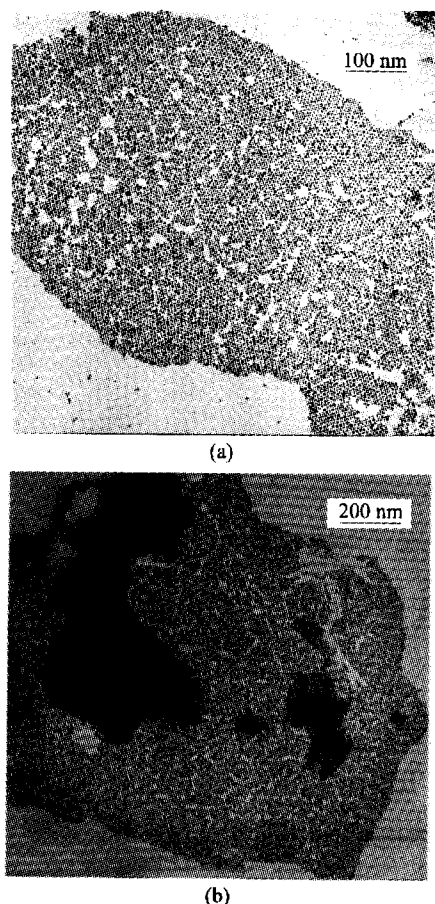


Fig. 8 TEM micrograph of $C_{12}H_{25}SH$ -capped gold nanoparticles obtained from toluene for the volume ratio of $C_{12}H_{25}SH/Au$ colloid $r = 1.0$. (a) large domain of 2D nanoarray, (b) large domain of 2D + 3D superstructure.

When $r = 1$ (volume ratio of $C_{12}H_{25}SH$ to Au colloid), a large domain of 2D nanoarray as well as 2D + 3D superstructures was observed. Fig. 8(a) and (b) show the TEM micrograph of the 2D and 2D + 3D of gold nanoparticles, respectively. In Fig. 8(a), a pure 2D array of gold nanoparticles as large as $1.0 \times 0.8 \mu m^2$ can be clearly seen. Some defects (voids) still exist in this

large area of 2D monolayer. Even larger of $1.6 \times 1.5 \mu m^2$ superlattice has also been observed, as shown in Fig. 8(b). In this case, the large area of 2D superstructure coexists with small area of 3D superlattice, which can be resolved clearly by the change of the contrast in this micrograph. Similar to Fig. 8(a), some voids are also present in this superstructure. It seems difficult to avoid these defects in the large area of superstructures. The same situation holds for the superlattices of other nanoparticles as reported before.^{3,5,10}

Conclusion

From this study it can be concluded that gold nanoparticles without ligands or without suitable ligands can not form well ordered superlattices because the surfaces of the particles are not well protected and passivated. It is shown that the alkanethiol (sulfide) with a long straight chain (C8, C12) can form a compact layer passivating the underlying spherical gold nanoparticles, which leads to the formation of ordered superstructures. The gold nanoparticles derived from CTAB micelle system and capped by dodecanethiol $C_{12}H_{25}SH$ can form 1D, 2D and 3D superlattices. Among them the 2D nanoarray is highly ordered and frequently observed. A relatively large domain of superstructure can be obtained by suitably adjusting the $C_{12}H_{25}SH/Au$ colloid volume ratio.

References

- Xia, Y.; Gates, B.; Yin, Y.; Lu, Y. *Adv. Mater.* **2000**, *12*, 693.
- Storhoff, J. J.; Mucic, R. C.; Mirkin, C. A. *J. Cluster Sci.* **1997**, *8*, 179.
- Wang, Z. L. *Adv. Mater.* **1998**, *10*, 13.
- Murray, C. B.; Kagan, C. R.; Bawendi, M. G. *Science* **1995**, *270*, 1335.
- Motte, L.; Billoudet, F.; Lacaze, E.; Douin, J.; Pileni, M. P. *J. Phys. Chem. B* **1997**, *101*, 138.
- Korgel, B. A.; Fitzmaurice, D. *Adv. Mater.* **1998**, *19*, 661.
- Harfenist, S. A.; Wang, Z. L.; Alvarez, M. A.; Vezmar, I.; Whetten, R. L. *J. Phys. Chem.* **1996**, *100*, 13904.
- Taleb, A.; Petit, C.; Pileni, M. P. *Chem. Mater.* **1997**, *9*, 950.
- Petit, C.; Taleb, A.; Pileni, M. P. *J. Phys. Chem. B*

- 1999, 103, 1805.
- 10 Sun, S.; Murray, C. B. *J. Appl. Phys.* **1999**, 85, 4325.
- 11 Hayat, M. A. *Colloid Gold: Principles, Methods and Applications*, Vol. 1, Academic Press, San Diego, **1989**, pp. 1—10.
- 12 Brust, M.; Walker, M.; Bethell, D.; Schiffrin, D. J.; Whyman, R. *J. Chem. Soc., Chem. Commun.* **1994**, 801.
- 13 Whetten, R. L.; Khoury, J. T.; Alvarez, M. M.; Murthy, S. *Adv. Mater.* **1996**, 8, 428.
- 14 Sarathy, K. V.; Kulkarni, G. U.; Rao, C. N. R. *J. Chem. Soc., Chem. Commun.* **1997**, 537.
- 15 Andres, R. P.; Bielfeld, J. D.; Henderson, J. I. *Science* **1995**, 273, 1690.
- 16 Spatz, J. P.; Moebner, S.; Moeller, M. *Chem. Eur. J.* **1997**, 2, 1552.
- 17 Kiely, C. J.; Fink, J.; Brust, M.; Bethell, D.; Schiffrin, D. J. *Nature* **1998**, 396, 444.
- 18 Barnickel, P.; Wokaun, A. *Mol. Phys.* **1990**, 1, 69.
- 19 Ayyub, P.; Maitra, A.; Shah, D. O. *J. Chem. Soc. Faraday Trans.* **1993**, 89, 3585.
- 20 Ulman, A. *Chem. Rev.* **1996**, 96, 1533.
- 21 Schmid, G.; Hornyak, G. L. *Curr. Opin. Solid State Mater. Sci.* **1997**, 2, 204.
- 22 Hostetler, M. J.; Stokes, J. J.; Murray, R. M. *Langmuir* **1996**, 12, 3604.
- 23 Fink, J.; Kiely, C. J.; Bethell, D.; Schiffrin, D. J. *Chem. Mater.* **1998**, 10, 922.

(E0109171 LI, L. T.; DONG, H. Z.)